

Mechanisms of Iron Porphyrin Reactions with Peroxynitrite

Jinbo Lee, Julianne A. Hunt, and John T. Groves*

Contribution from the Department of Chemistry, Princeton University, Princeton, New Jersey 08544

Received February 16, 1998

Abstract: Peroxynitrite (ONOO^-) is a major cytotoxic agent that has been implicated in a host of pathophysiological conditions; it is therefore important to develop therapeutic agents to detoxify this potent biological oxidant, and to understand the modes of action of these agents. Water-soluble iron porphyrins, such as 5,10,15,20-tetrakis(*N*-methyl-4'-pyridyl)porphyrinatoiron(III) [Fe(III)TMPyP] and 5,10,15,20-tetrakis-(2,4,6-trimethyl-3,5-sulfonatophenyl)porphyrinatoiron(III) [Fe(III)TMPS], have been shown to catalyze the efficient decomposition of ONOO^- to NO_3^- and NO_2^- under physiological conditions. However, the mechanisms of ONOO^- decomposition catalyzed by these water-soluble iron porphyrins have not yet been elucidated. We have shown that there are two different pathways operating in the catalytic decomposition of ONOO^- by FeTMPyP. Fe(III)TMPyP reacts rapidly with ONOO^- to produce oxoFe(IV)TMPyP and NO_2 ($k \approx 5 \times 10^7 \text{ M}^{-1} \text{ s}^{-1}$). The oxoFe(IV) porphyrin, which persisted throughout the catalytic decomposition of ONOO^- , was shown to be relatively unreactive toward NO_2 and NO_2^- . This oxoFe(IV) porphyrin was also shown to react with ONOO^- ($k = 1.8 \times 10^6 \text{ M}^{-1} \text{ s}^{-1}$), and it was this oxoFe(IV)- ONOO^- reaction pathway that predominated under conditions of excess ONOO^- with respect to Fe(III)TMPyP. The competition between the two pathways explains the highly nonlinear relationship observed for k_{cat} with respect to ONOO^- concentration. Fe(III)TMPyP is also known to catalyze the dismutation of the ONOO^- precursor superoxide ($\text{O}_2^{\bullet-}$), and using stopped-flow spectrophotometry, the rate of Fe(III)TMPyP-catalyzed $\text{O}_2^{\bullet-}$ dismutation has been determined to be $1.9 \times 10^7 \text{ M}^{-1} \text{ s}^{-1}$ by direct measurement. A detailed mechanistic understanding of how iron porphyrins function in the catalytic decomposition of both ONOO^- and $\text{O}_2^{\bullet-}$ may prove essential in the exploration of the chemistry and biology of these reactive oxygen species, and in understanding the biological activity of these metalloporphyrins.

Introduction

Peroxynitrite (ONOO^-) is a potent cytotoxic agent formed by the direct and rapid combination of nitric oxide and the superoxide anion ($\text{O}_2^{\bullet-}$).^{1–3} A strong one- and two-electron oxidant, ONOO^- has been shown to react with a wide variety of biomolecules, including proteins (via nitration of tyrosine^{4,5} and tryptophan^{6,7} residues, oxidation of methionine⁸ and selenocysteine⁹ residues, and oxidation of metalloenzymes^{10,11}), DNA,^{12,13} lipids,¹⁴ and antioxidants.^{15,16} We have recently demonstrated that ONOO^- crosses lipid membranes at a rate significantly faster than the rates of its known decomposition pathways.¹⁷ Thus ONOO^- , unlike reactive radicals such as $\text{O}_2^{\bullet-}$

or HO^\bullet , can travel distances of cellular dimensions and should have free access to cell interiors, even in the presence of biological membranes. There is mounting evidence that reactive oxygen and nitrogen species play important roles in the regulation and inhibition of mitochondrial respiration¹⁸ and in apoptosis,^{19,20} recent studies have shown that ONOO^- in particular is involved in apoptotic cell death in leukemia cells,^{21,22} aortic smooth muscle cells,²³ and neural cells.²⁴ In light of its high reactivity with biological targets, and possibly connected with its proposed role in the regulation of mitochondrial respiration and cellular apoptosis, ONOO^- has been implicated in a host of disease states, including neurodegen-

* To whom correspondence should be addressed. Phone: (609) 258-3593. Fax: (609) 258-0348.

(1) Beckman, J. S.; Beckman, T. W.; Chen, J.; Marshall, P. A.; Freeman, B. A. *Proc. Natl. Acad. Sci. U.S.A.* **1990**, *87*, 1620–1624.

(2) Huie, R. E.; Padmaja, S. *Free Radical Res. Commun.* **1993**, *18*, 195–199.

(3) Blough, N. V.; Zafiriou, O. C. *Inorg. Chem.* **1985**, *24*, 3504–3505.

(4) Ischiropoulos, H.; Zhu, L.; Chen, J.; Tsai, M.; Martin, J. C.; Smith, C. D.; Beckman, J. S. *Arch. Biochem. Biophys.* **1992**, *298*, 431–437.

(5) Beckman, J. S.; Ischiropoulos, H.; Zhu, L.; Woerd, M. V. D.; Smith, C.; Chen, J.; Harrison, J.; Martin, J. C.; Tsai, M. *Arch. Biochem. Biophys.* **1992**, *298*, 438–445.

(6) Alvarez, B.; Rubbo, H.; Kirk, M.; Barnes, S.; Freedman, B. A.; Radi, R. *Chem. Res. Toxicol.* **1996**, *9*, 390–396.

(7) Padmaja, S.; Ramezani, M. S.; Bounds, P. L.; Koppenol, W. H. *Redox. Rep.* **1996**, *2*, 173–177.

(8) Pryor, W. A.; Jin, X.; Squadrito, G. L. *Proc. Natl. Acad. Sci. U.S.A.* **1994**, *91*, 11173–11177.

(9) Padmaja, S.; Squadrito, G. L.; Pryor, W. A. *Arch. Biochem. Biophys.* **1998**, *349*, 1–6.

(10) Floris, R.; Piersma, R.; Yang, G.; Jones, P.; Wever, R. *Eur. J. Biochem.* **1993**, *215*, 767–775.

(11) Castro, L.; Rodriguez, M.; Radi, R. *J. Biol. Chem.* **1994**, *269*, 29409–29415.

(12) King, P. A.; Anderson, V. E.; Edwards, J. O.; Gustafson, G.; Plumb, R. C.; Suggs, J. W. *J. Am. Chem. Soc.* **1992**, *114*, 5430–5432.

(13) King, P. A.; Jamison, E.; Strahs, D.; Anderson, V. E.; Brenowitz, M. *Nucleic Acids Res.* **1993**, *21*, 2473–2478.

(14) Radi, R.; Beckman, J. S.; Bush, K. M.; Freeman, B. A. *Arch. Biochem. Biophys.* **1991**, *288*, 481–487.

(15) Radi, R.; Beckman, J. S.; Bush, K. M.; Freeman, B. A. *J. Biol. Chem.* **1991**, *266*, 4244–4250.

(16) Bartlett, D.; Church, D. F.; Bounds, P. L.; Koppenol, W. H. *Free Radical Biol. Med.* **1995**, *18*, 85–92.

(17) Marla, S. S.; Lee, J.; Groves, J. T. *Proc. Natl. Acad. Sci. U.S.A.* **1997**, *94*, 14243–14248.

(18) Ghafourifar, P.; Richter, C. *FEBS Lett.* **1997**, *418*, 291–296.

(19) Review: Richter, C. *Biosci. Rep.* **1997**, *17*, 53–66.

(20) Polyak, K.; Xia, Y.; Zweier, J. L.; Kinzler, K. W.; Vogelstein, B. *Nature* **1997**, *389*, 300–305.

(21) Lin, K.-T.; Xue, J.-Y.; Nomen, M.; Spur, B.; Wong, P. Y.-K. *J. Biol. Chem.* **1995**, *270*, 16487–16490.

(22) Lin, K.-T.; Xue, J.-Y.; Sun, F. F.; Wong, P. Y.-K. *Biochem. Biophys. Res. Commun.* **1997**, *230*, 115–119.

(23) O'Connor, M.; Salzman, A. L.; Szabo, C. *Shock* **1997**, *8*, 439–443.

(24) Keller, J. N.; Kindy, M. S.; Holtsberg, F. W.; St. Clair, D. K.; Yen, H. C.; Germeyer, A.; Steiner, S. M.; Bruce-Keller, A. J.; Hutchins, J. B.; Mattson, M. P. *J. Neurosci.* **1998**, *18*, 687–697.

erative disorders,^{25–38} heart diseases,^{39,40} chronic inflammation and autoimmune diseases,^{41–44} cancer,^{45–47} ischemia-reperfusion injury,^{1,48–51} and septic shock.⁵² This large and rapidly expanding body of evidence on the role of ONOO⁻ in a wide variety of human diseases has naturally led to a search for drugs that can intercept this powerful oxidant.

We have recently shown that ONOO⁻ reacts rapidly and stoichiometrically with the water-soluble synthetic manganese porphyrin 5,10,15,20-tetrakis(*N*-methyl-4'-pyridyl)porphinato-manganese(III) [Mn(III)TMPyP] to generate oxomanganese intermediates.^{17,53} Mn(III)TMPyP catalyzed the rapid reduction of ONOO⁻ in the presence of biological antioxidants, such as ascorbate, glutathione, and Trolox (a water-soluble analogue of α -tocopherol).⁵⁴ In addition to this "peroxynitrite reductase" activity, Mn(III)TMPyP has been shown to possess significant activity for the simultaneous oxidation of superoxide (O₂^{-•}) and reduction of ONOO⁻.⁵⁵ Furthermore, amphiphilic analogues of Mn(III)TMPyP have been prepared which proved to be effective ONOO⁻ decomposition catalysts in liposomal assemblies.⁵⁶ The fast catalytic turnover of both the water-soluble

Mn(III)TMPyP and its amphiphilic analogues requires the presence of biological antioxidants, and the concentrations of these antioxidants might be low under conditions of oxidative stress, when the levels of prooxidants and antioxidants are not in balance.^{57,58} Thus, it is highly desirable to develop ONOO⁻ decomposition catalysts that function even in the absence biological antioxidants.

Stern *et al.*⁵⁹ have shown that 5,10,15,20-tetrakis(*N*-methyl-4'-pyridyl)porphinatoiron(III) [Fe(III)TMPyP] and 5,10,15,20-tetrakis(2,4,6-trimethyl-3,5-sulfonatophenyl)porphinatoiron(III) [Fe(III)TMPS] display profound activity in biological models of ONOO⁻ related disease states and have been investigated as therapeutic agents for diseases in which ONOO⁻ has been implicated.^{59–62} These iron porphyrins were proposed to possess catalytic "peroxynitrite isomerase" activity, converting ONOO⁻ to NO₃⁻. However, a consensus has not yet been reached on the mechanism of ONOO⁻ decomposition catalyzed by these iron porphyrins.

Herein we elaborate on the reactions of Fe(III)TMPyP with ONOO⁻. Significantly, both Fe(III)TMPyP and oxoFe(IV)-TMPyP have been found to react with ONOO⁻ under typical catalytic conditions, which accounts for the significant difference in activity between iron and manganese porphyrins toward peroxynitrite. In addition, we have studied the SOD activity of Fe(III)TMPyP. As we have recently described for Mn(III)-TMPyP,⁵⁵ the SOD activity of Fe(III)TMPyP may be accompanied by a O₂^{-•}-coupled ONOO⁻ reductase pathway. The simultaneous and redox-coupled removal of O₂^{-•} and ONOO⁻ by Fe(III)TMPyP may explain the remarkable biological activity of this and other iron porphyrins.

Results and Discussion

Elucidation of the mechanism of ONOO⁻ isomerization catalyzed by water-soluble iron porphyrins such as Fe(III)-TMPyP and Fe(III)TMPS depends on the identification of the reactive intermediates and on the development of an understanding of the reaction kinetics. Peroxynitrite, the anion of peroxynitrous acid (ONOOH), is expected to react as a typical peroxide, and reactions of peroxides with iron porphyrins and heme-dependent enzymes are known to produce reactive oxoiron intermediates.^{63–68} For example, compound I of the peroxidase enzymes has been described as an oxoFe(IV) porphyrin cation radical, while compound II has been described as an oxoFe(IV) species.^{69–73} An oxoFe(IV) porphyrin cation radical, analogous to compound I of the peroxidases but with a thiolate axial ligand, is believed to be the active intermediate in various reactions⁶³ catalyzed by the family of cytochrome P450 enzymes.⁷⁴ For iron porphyrin model systems, both the oxoFe(IV) porphyrin cation radical and the oxoFe(IV) species have been isolated and well-characterized.^{75,76} The reaction of

(52) Szabo, C.; Salzman, A. L.; Ischiropoulos, H. *FEBS Lett.* **1995**, *363*, 235–238.

(53) Groves, J. T.; Marla, S. S. *J. Am. Chem. Soc.* **1995**, *117*, 9578–9579.

(54) Lee, J.; Hunt, J. A.; Groves, J. T. *Bioorg. Med. Chem. Lett.* **1997**, *7*, 2913–2918.

(55) Lee, J.; Hunt, J. A.; Groves, J. T. *J. Am. Chem. Soc.* **1998**, *120*, 6053–61.

(56) Hunt, J. A.; Lee, J.; Groves, J. T. *Chem. Biol.* **1997**, *4*, 845–858.

(57) Scandalios, J. G. *Oxidative Stress and the Molecular Biology of Antioxidant Defenses*; Cold Spring Harbor Laboratory Press: New York, 1997.

(58) Sies, H. *Oxidative Stress*; Academic Press: Orlando, FL, 1985.

(59) Stern, M. K.; Jensen, M. P.; Kramer, K. *J. Am. Chem. Soc.* **1996**, *118*, 8735–8736.

(60) Stern, M. K.; Salvemini, D. *PCT Int. Appl. WO95/31197*, 1995.

(61) Salvemini, D.; Wang, Z.-Q.; Bourdon, D. M.; Stern, M. K.; Currie, M. G.; Manning, P. T. *Eur. J. Pharmacol.* **1996**, *303*, 217–220.

(62) Salvemini, D.; Wang, Z. Q.; Stern, M. K.; Currie, M. G.; Misko, T. P. *Proc. Natl. Acad. Sci. U.S.A.* **1998**, *95*, 2659–2663.

(25) Lipton, S. A.; Chol, T.-B.; Pan, Z.-H.; Lei, S. Z.; Chen, H.-S.; Sucher, N. J.; Loscalzo, J.; Singel, D. J.; Stamler, J. S. *Nature* **1993**, *364*, 626–631.

(26) Good, P. F.; Werner, P.; Hsu, A.; Olanow, C. W.; Perl, D. P. *Am. J. Pathol.* **1996**, *149*, 21–28.

(27) Matthews, R. T.; Beal, M. F. *Brain Res.* **1996**, *718*, 181–184.

(28) Bonfoco, E.; Krainc, D.; Ankarcrona, M.; Nicotera, P.; Lipton, S. A. *Proc. Natl. Acad. Sci. U.S.A.* **1995**, *92*, 7162–7166.

(29) Beckman, J. S.; Carson, M.; Smith, C. D.; Koppenol, W. H. *Nature* **1993**, *364*, 584.

(30) Rosen, D. R.; et al.; Brown, R. H. *Nature* **1993**, *352*, 59–62.

(31) Wiedau-Pazos, M.; Goto, J. J.; Rabizadeh, S.; Gralla, E. B.; Roe, J. A.; Lee, M. K.; Valentine, J. S.; Bredesen, D. E. *Science* **1996**, *271*, 515–518.

(32) Deng, H. X.; Hentati, A.; Tainer, J. A.; Iqbal, Z.; Cayabyab, A.; Hung, W. Y.; Getzoff, E. D.; Hu, P.; Herzfeldt, B.; Roos, R. P.; Warner, C.; Deng, G.; Soriano, E.; Smyth, C.; Parge, H. E.; Ahmed, A.; Roses, A. D.; Hallewell, R. A.; Pericak-Vance, M. A.; Siddique, T. *Science* **1993**, *261*, 1047–1051.

(33) Crow, J. P.; Sampson, J. B.; Zhuang, Y. X.; Thompson, J. A.; Beckman, J. S. *J. Neurochem.* **1997**, *69*, 1936–1944.

(34) Dawson, V. L.; Dawson, T. M. *J. Chem. Neuroanat.* **1996**, *10*, 179–190.

(35) Szabo, C. *Free Radical Biol. Med.* **1996**, *21*, 855–869.

(36) Zhang, J.; Dawson, V. L.; Dawson, T. M.; Snyder, S. H. *Science* **1994**, *263*, 687–689.

(37) Adamson, D. C.; Wildermann, B.; Sasaki, M.; Glass, J. D.; McArthur, J. C.; Christov, V. I.; Dawson, T. M.; Dawson, V. L. *Science* **1996**, *274*, 1917–1921.

(38) Lipton, S. A.; Rosenberg, P. A. *New Engl. J. Med.* **1994**, *330*, 613–622.

(39) White, C. R.; Brock, T. A.; Chang, L.; Crapo, J.; Briscoe, P.; Ku, D.; Bradley, W. A.; Gianturco, S. H.; Gore, J.; Freeman, B. A.; Tarpey, M. M. *Proc. Natl. Acad. Sci. U.S.A.* **1994**, *91*, 1044–1048.

(40) Shimojo, T.; Nishiwaka, T.; Ishiyama, S.; Ikeda, I.; Kasajima, T.; Marumo, F.; Hiroe, M. *Cardiovasc. Pathol.* **1998**, *7*, 25–30.

(41) Kaur, H.; Halliwell, B. *FEBS Lett.* **1994**, *350*, 9–12.

(42) Rachmilewitz, D.; Stamler, J. S.; Karmeli, F.; Mullins, M. E.; Singel, D. J.; Loscalzo, J.; Xavier, R. J.; Podolski, D. K. *Gastroenterology* **1993**, *105*, 1681–1688.

(43) Seo, H. G.; Takata, I.; Nakamura, M.; Tatsumi, H.; Suzuki, K.; Fujii, J.; Taniguchi, N. *Arch. Biochem. Biophys.* **1995**, *324*, 41–47.

(44) Haddad, I. Y.; Pataki, G.; Hu, P.; Beckman, J. S.; Matalon, S. J. *Clin. Invest.* **1994**, *94*, 2407–2413.

(45) Mannick, E. E.; Bravo, L. E.; Zarama, G.; Realpe, J. L.; Zhang, X. J.; Ruit, B.; Fonham, E. T. H.; Mera, R.; Miller, M. J. S.; Coprea, P. *Cancer Res.* **1996**, *56*, 3238–3243.

(46) Douki, T.; Cadet, J.; Ames, B. N. *Chem. Res. Toxicol.* **1996**, *9*, 3–7.

(47) Juedes, M. J.; Wogan, G. N. *Mutation Res.* **1996**, *349*, 51–61.

(48) Chan, P. H. *Stroke* **1996**, *27*, 1124–1129.

(49) Huang, Z.; Huang, P. L.; Panahian, N.; Dalkara, T.; Fishman, M. C.; Moskowitz, M. A. *Science* **1994**, *265*, 1883–1885.

(50) Ma, X. L.; Lopez, B. L.; Liu, G. L.; Christopher, T. A.; Ischiropoulos, H. *Cardiovasc. Res.* **1997**, *36*, 1195–204.

(51) Alayash, A. I.; Ryan, B. A. B.; Cashon, R. E. *Arch. Biochem. Biophys.* **1998**, *349*, 65–73.

ONOO⁻ with horseradish peroxidase has been shown to produce compound I,^{10,77} while it is the compound II analogue that has been observed under conditions of catalytic turnover with Fe(III)TMPyS.⁵⁹

Our studies of the catalytic mechanism of ONOO⁻ isomerization by Fe(III)TMPyP thus began with an investigation of reactive oxoFe intermediates. The generation of oxoFe intermediates by ONOO⁻ and analogous peroxides, such as *m*-CPBA and HSO₅⁻, was explored with use of rapid-mixing stopped-flow spectrophotometry.

Detection of Reactive Intermediates. The stoichiometric reaction of 5 μM Fe(III)TMPyP and 5 μM *m*-CPBA produced an oxidized iron porphyrin intermediate with a Soret maximum at 427 nm, as monitored by time-resolved UV-vis spectroscopy (Figure 1a). This intermediate then decayed slowly back to Fe(III)TMPyP (λ_{max} = 423 nm). The spectrum of the observed intermediate and the spectral change in the conversion of this intermediate back to Fe(III)TMPyP are nearly identical to those of well-studied oxoFe(IV) porphyrin intermediates of other water-soluble iron porphyrins.^{59,78} Thus, we formulate the intermediate as an oxoFe(IV) species.^{79–82} Though isosbestic points around 410, 448, 522, and 568 nm can be identified in the conversion of this oxoFe(IV) species back to Fe(III)TMPyP, the stoichiometric reaction of Fe(III)TMPyP and *m*-CPBA resulted in significant destruction of the porphyrin chromophore (bleaching), with only 62% of the Fe(III)TMPyP recovered after the reaction (Figure 1a, inset).

One equivalent of nitrite (NO₂⁻) in an otherwise identical reaction mixture protected most of the Fe(III)TMPyP from bleaching (Figure 1a, inset). Furthermore, the isosbestic points were better defined in the time-resolved UV-vis spectra when

(63) Groves, J. T.; Han, Y.-Z. *Models and Mechanisms of Cytochrome P450 Action*; Ortiz de Montellano, P. R., Ed.; Plenum Press: New York, 1995; pp 3–48.

(64) Sheldon, R. A.; Kochi, J. K. *Metal Catalyzed Oxidations of Organic Compounds*; Academic Press: New York, 1981.

(65) Hill, C. L. *Activation and functionalization of alkanes*; John Wiley & Sons: New York, 1989.

(66) Davies, J. A., et al. *Selective Hydrocarbon Activation: Principle and Progress*; VCH: New York, 1994.

(67) Sheldon, R. A. *Metalloporphyrins in Catalytic Oxidations*; M. Dekker: New York, 1994.

(68) (a) *Metalloporphyrin Catalyzed Oxidations*; Montanari, F., Casella, L., Eds.; Kluwer: Dordrecht, The Netherlands, 1994. (b) Meunier, B. *Chem. Rev.* **1992**, *92*, 1411–56. Dolphin, D.; Traylor, T. G.; Xie, L. Y. *Acc. Chem. Res.* **1997**, *30*, 251–59.

(69) Mann, T. *Oxidases and Related Redox Systems*; King, T. E., Mason, H. S., Morrison, M., Eds.; Liss: New York, 1988; pp 29–49.

(70) Dolphin, D.; Forman, A.; Borg, D. C.; Fayer, J.; Felton, R. H. *Proc. Natl. Acad. Sci. U.S.A.* **1971**, *68*, 614–618.

(71) Dolphin, D.; Felton, R. H. *Acc. Chem. Res.* **1974**, *7*, 26–32.

(72) Peisach, J.; Blumberg, W. E.; Wittenberg, B. A.; Wittenberg, J. B. *J. Biol. Chem.* **1968**, *243*, 1871–1880.

(73) Penner-Hahn, J. E.; McMurry, T. J.; Renner, M.; Latos-Grazynski, L.; Eble, K. S.; Davis, I. M.; Balch, A. L.; Groves, J. T.; Dawson, J. R.; Hodgson, K. O. *J. Biol. Chem.* **1983**, *258*, 12761–12764.

(74) Dawson, J. H.; Eble, K. S. *Adv. Inorg. Bioinorg. Mech.* **1986**, *4*, 1–64.

(75) Groves, J. T.; Haushalter, R. C.; Nakamura, M.; Nemo, T. E.; Evans, B. J. *J. Am. Chem. Soc.* **1981**, *102*, 2884–2886.

(76) Groves, J. T.; Gross, Z.; Stern, M. K. *Inorg. Chem.* **1994**, *33*, 5065–5072.

(77) Floris, R.; Piersma, S. R.; Yang, G.; Jones, P.; Wever, R. *Eur. J. Biochem.* **1993**, *215*, 767–75.

(78) Colclough, N.; Smith, J. R. L. *J. Chem. Soc., Perkin Trans. 2* **1994**, 1139–1149.

(79) Chen, S.-M.; Su, Y. O. *J. Chem. Soc., Chem. Commun.* **1990**, 491–493.

(80) Rodgers, K. R.; Reed, R. A.; Su, Y. O.; Spiro, T. G. *Inorg. Chem.* **1992**, *31*, 2688–2700.

(81) Mn(III)/Mn(IV) porphyrin redox potentials are higher than corresponding values for iron, cf.: Kaaret, T. W.; Zhang, G.-H.; Bruce, T. C. *J. Am. Chem. Soc.* **1991**, *113*, 4652–4656.

(82) Jeon, S.; Bruce, T. C. *Inorg. Chem.* **1992**, *31*, 4843–4848.

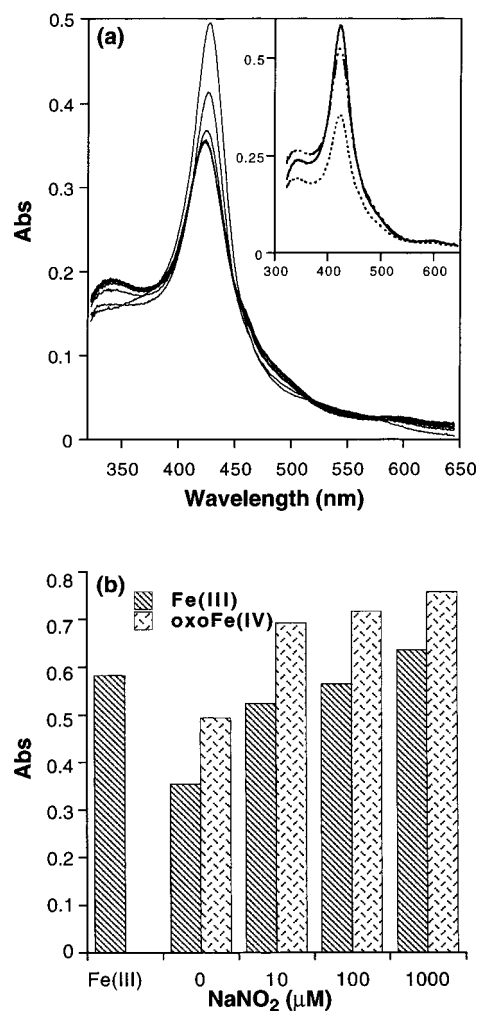
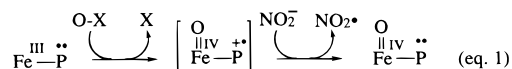


Figure 1. (a) Time-resolved UV-vis spectra of the stoichiometric reaction of 5 μM Fe(III)TMPyP with 5 μM *m*-CPBA in 25 mM phosphate pH 7.4 buffer. The decay of the oxoFe(IV) intermediate back to Fe(III)TMPyP is shown. The reaction was followed by UV-vis spectroscopy (100 scans in 60 s, 0.005 s integration time) with a stopped-flow spectrophotometer (1 in 10 scans shown for clarity). Inset: Solid trace, Fe(III)TMPyP (5 μM); lower dotted trace, recovered Fe(III)TMPyP (5 μM) after reaction with *m*-CPBA (5 μM); middle dotted trace, recovered Fe(III)TMPyP (5 μM) after reaction with *m*-CPBA (5 μM) in the presence of NaNO₂ (5 μM). (b) Dependence of the extent of oxoFe(IV) formation and Fe(III)TMPyP recovery on NaNO₂ concentration in the reaction of 5 μM Fe(III)TMPyP with 5 μM *m*-CPBA. Fe(III)TMPyP and the oxoFe(IV) species were monitored at 423 and 427 nm, respectively. The first column on the left represents 5 μM Fe(III)TMPyP with no added *m*-CPBA or NaNO₂.

1 equiv of NO₂⁻ was present (data not shown). In fact, addition of NO₂⁻ to the stoichiometric reaction mixture of Fe(III)TMPyP and *m*-CPBA not only increased the yield of recovered Fe(III)TMPyP, but also enhanced the level of the oxoFe(IV) porphyrin intermediate formed (Figure 1b). Taken together, these data suggest the presence of an intermediate more reactive toward bleaching than oxoFe(IV); this intermediate can be reduced rapidly by NO₂⁻, and this reduction protects the porphyrin from oxidative destruction. Thus, the overall reaction, presented in eq 1, involves oxidation of Fe(III)TMPyP to a reactive porphyrin intermediate, which is then reduced by NO₂⁻ to an oxoFe(IV) species.



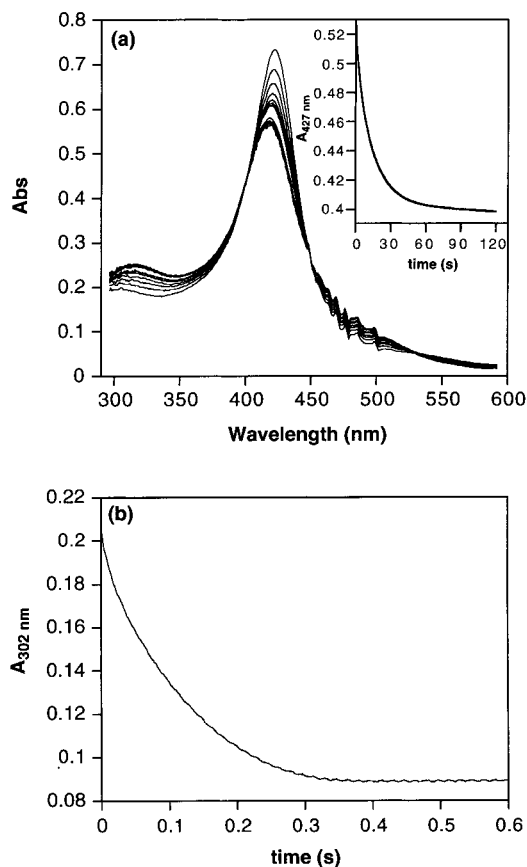
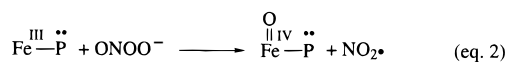


Figure 2. (a) Time-resolved UV-vis spectra of the reaction of 5 μM Fe(III)TMPyP with 100 μM ONOO $^-$ in 25 mM phosphate buffer at pH 7.4, 25 $^\circ\text{C}$. The decay of the oxoFe(IV) intermediate back to Fe(III)TMPyP is shown. The reaction was followed by UV-vis spectroscopy (100 scans in 30 s, 0.005 s integration time) with a stopped-flow spectrophotometer (for clarity, every other scan is shown for the first 10 scans, and thereafter every tenth scan is shown). Inset: Decay of the oxoFe(IV) species back to Fe(III)TMPyP monitored at 427 nm. (b) Decomposition of 100 μM ONOO $^-$ catalyzed by 5 μM Fe(III)TMPyP. The decay of ONOO $^-$ was monitored at 302 nm.

This fast reduction of a reactive iron porphyrin intermediate by NO $_2^-$ is highly analogous to the reduction of oxoMn(V)TMPyP by NO $_2^-$, which is known to be rapid and quantitative.⁸³ Possible candidates for the reactive iron intermediate thus include the oxoFe(IV) porphyrin cation radical (as shown in eq 1)⁷⁵ or an oxoFe(V) species.

Similarly, ONOO $^-$ oxidized Fe(III)TMPyP to the same oxoFe(IV) porphyrin species at concentrations as low as 1 equiv, simultaneously producing 1 equiv of NO $_2$, as monitored by time-resolved UV-vis spectroscopy (eq 2).



Data for the reaction of Fe(III)TMPyP with excess ONOO $^-$ are shown in Figure 2a; analogous results were obtained in the stoichiometric reaction (data not shown). The formation of the oxoFe(IV) species and NO $_2$ could be achieved either by homolysis of the bound ONOO $^-$ or heterolysis followed by fast reduction of the oxoFe(IV) porphyrin cation radical [or the oxoFe(V) species] by NO $_2^-$ in the solvent cage. Surprisingly, the oxoFe(IV) porphyrin intermediate persisted even in the presence of NO $_2$, and then slowly returned to Fe(III)TMPyP

(83) Groves, J. T.; Lee, J.; Marla, S. S. *J. Am. Chem. Soc.* **1997**, *119*, 6269–6273.

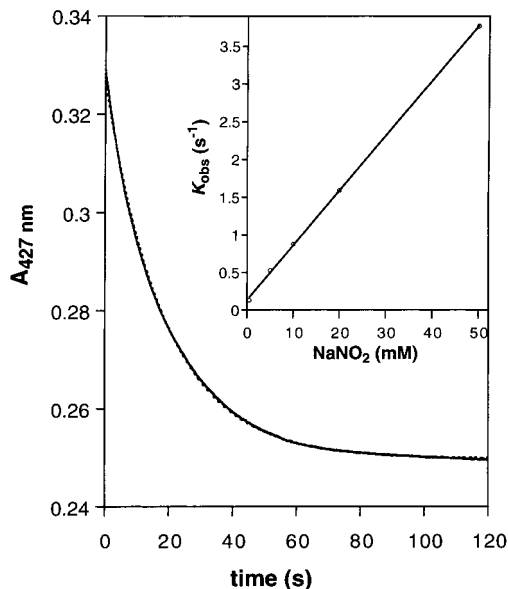


Figure 3. The decay of the oxoFe(IV) species back to Fe(III)TMPyP is a first-order process. The kinetic trace shown was obtained from a double-mixing stopped-flow experiment, in which the oxoFe(IV) species was generated by reaction of 5 μM Fe(III)TMPyP with 5 μM HSO $_5^-$ in the first-mixing step, and 50 mM pH 7.4 phosphate buffer was added in the second-mixing step. The experimental data nicely fit a single-exponential curve, giving a first-order rate constant of $k = 0.053 \text{ s}^{-1}$ ($R = 0.999$). Inset: Slow reduction of the oxoFe(IV) species by NaNO $_2$, with a second-order rate constant of $k = 73 \text{ M}^{-1} \text{ s}^{-1}$ ($R = 0.999$).

over the period of a minute (Figure 2a, inset), as in the *m*-CPBA reaction shown above. This observation indicates that the recombination of oxoFe(IV)TMPyP and NO $_2$ is a slow process, which cannot be the major contributor to the catalytic turnover in Fe(III)TMPyP catalyzed decomposition of ONOO $^-$. When 5 μM Fe(III)TMPyP reacted with 100 μM ONOO $^-$, the oxoFe(IV) species persisted throughout the decay of ONOO $^-$ monitored at 302 nm (compare Figure 2b with Figure 2a, inset). After ONOO $^-$ was fully decomposed, the oxoFe(IV) species then started its typical slow decay back to Fe(III)TMPyP (Figure 2a, inset). Again, these results suggest that oxoFe(IV)TMPyP cannot be the transient intermediate in the turnover of Fe(III)TMPyP-catalyzed decomposition of ONOO $^-$. Thus, we set out to determine the role of the oxoFe(IV) species in the catalytic decomposition of ONOO $^-$.

The Role of OxoFe(IV) in Peroxynitrite Decomposition.

The oxoFe(IV) intermediate generated by ONOO $^-$ and *m*-CPBA was also generated by reaction of Fe(III)TMPyP with HSO $_5^-$, but at a slower rate. This is consistent with the trend in oxidation rates we previously observed in the reactions of Mn(III)TMPyP with *m*-CPBA, ONOO $^-$, and HSO $_5^-$.⁸³ The second-order rate constant for the reaction of Fe(III)TMPyP with HSO $_5^-$ is $2.1 \times 10^5 \text{ M}^{-1} \text{ s}^{-1}$, obtained from a linear plot of the apparent first-order rate constants, k_{obs} , against the HSO $_5^-$ concentrations.⁸⁴ The oxoFe(IV) species generated by this reaction was fairly stable, decaying slowly back to Fe(III)TMPyP with a first-order rate constant of 0.053 s^{-1} (Figure 3). Not only was the recombination of oxoFe(IV) and NO $_2$ a slow process, as discussed above, but the reduction of oxoFe(IV) by NO $_2^-$ was also found to be slow, with a second-order rate

(84) The second-order rate constant for the oxidation of Fe(III)TMPyP by HSO $_5^-$ was determined from the following data points: 50 μM HSO $_5^-$, $k_{\text{obs}} = 10.4 \text{ s}^{-1}$; 75 μM HSO $_5^-$, $k_{\text{obs}} = 15.1 \text{ s}^{-1}$; 100 μM HSO $_5^-$, $k_{\text{obs}} = 20.5 \text{ s}^{-1}$; 125 μM HSO $_5^-$, $k_{\text{obs}} = 26.6 \text{ s}^{-1}$; 150 μM HSO $_5^-$, $k_{\text{obs}} = 31.6 \text{ s}^{-1}$; $R = 0.999$.

constant of $73 \text{ M}^{-1} \text{ s}^{-1}$ (Figure 3, inset).⁸⁵ The stability of the oxoFe(IV)TMPyP species and its low reactivity toward NO_2^- are, again, analogous to the stability and low reactivity of the corresponding oxoMn(IV) porphyrin intermediate,⁸³ which is known to be unable to catalyze decomposition of ONOO^- .^{17,54}

Thus, we were surprised to discover that the oxoFe(IV) species generated independently by reaction of Fe(III)TMPyP with HSO_5^- was active in decomposing ONOO^- . In a double-mixing experiment, the oxoFe(IV) species was generated by the stoichiometric reaction of $5 \mu\text{M}$ Fe(III)TMPyP and $5 \mu\text{M}$ HSO_5^- in the first mixing step; then $100 \mu\text{M}$ ONOO^- was added in the second mixing step. The kinetic profile for ONOO^- decay catalyzed by the oxoFe(IV) species was observed to be indistinguishable from that of the ONOO^- decay in the direct mixing of Fe(III)TMPyP and ONOO^- (Figure 4a). Thus, the oxoFe(IV) porphyrin intermediate, and not Fe(III)TMPyP, must be the major species catalyzing the isomerization of ONOO^- under these conditions. In fact, the rate of ONOO^- decomposition was not linearly dependent on the Fe(III)TMPyP concentration in a series of experiments in which the concentration of ONOO^- was kept constant while the concentration of Fe(III)TMPyP was varied. Instead, an upward parabolic relationship was found (Figure 4b). When the concentration of ONOO^- was much higher than the concentration of iron catalyst (reaction under pseudo-first-order conditions), the rate of ONOO^- decay was almost linearly dependent on the concentration of Fe(III)TMPyP. A catalytic rate constant (k_{cat}) was estimated to be around $1.8 \times 10^6 \text{ M}^{-1} \text{ s}^{-1}$ under these conditions, consistent with that estimated by Stern *et al.*⁵⁹

However, the rate of ONOO^- decomposition became much faster, and deviated significantly from a linear relationship, when the concentration of ONOO^- was comparable to that of Fe(III)TMPyP and the reaction was thus no longer under pseudo-first-order conditions (Figure 4b). This clearly indicates a change of mechanism for ONOO^- decomposition as the relative concentrations of ONOO^- and Fe(III)TMPyP were changed. Interestingly, this nonlinear relationship is similar to the observation by Stern *et al.*, for a series of experiments in which the concentration of Fe(III)TMPyP was held constant while the concentration of ONOO^- was varied.⁵⁹ Further, the catalytic rate constant of ONOO^- decomposition catalyzed by Fe(III)TMPyP in the presence of ascorbate ($k_{\text{cat}} > 10^7 \text{ M}^{-1} \text{ s}^{-1}$)⁸⁶ was significantly faster than that in the absence of ascorbate ($k_{\text{cat}} \sim 2.2 \times 10^6 \text{ M}^{-1} \text{ s}^{-1}$),⁵⁹ which again indicates a change of mechanism between these two processes. Finally, the catalytic decomposition of ONOO^- at near stoichiometric concentrations ($10 \mu\text{M}$) was almost 10 times faster than the catalytic decomposition of ONOO^- under pseudo-first-order conditions ($100 \mu\text{M}$), though the concentrations of the catalyst, Fe(III)TMPyP ($5 \mu\text{M}$), were the same in both reactions (Figure 5).

Clearly the Fe(III)TMPyP-catalyzed decomposition of ONOO^- is a complicated process. However, all the results presented above are consistent with the simplified mechanism shown in Scheme 1, in which two interconnected catalytic processes are proposed: A fast pathway (path 1) involves Fe(III)TMPyP as a stoichiometric reactant, while a 10-fold slower pathway (path 2) involves an oxoFe(IV) species as the active catalyst.

Mechanism of Fe(III)TMPyP-Catalyzed ONOO^- Decomposition. In the first and faster process (Scheme 1, path 1), ONOO^- reacts with Fe(III)TMPyP to produce oxoFe(IV) and

(85) As observed by Stern *et al.* (ref 59), unlike the oxoFe(IV) species of the cationic porphyrin FeTMPyP, the corresponding oxoFe(IV) species of the anionic porphyrin FeTMPS is rapidly reduced to Fe(III) by NO_2^- . We thank M. K. Stern for a gift of FeTMPS.

(86) Stern, M. K. Personal communication.

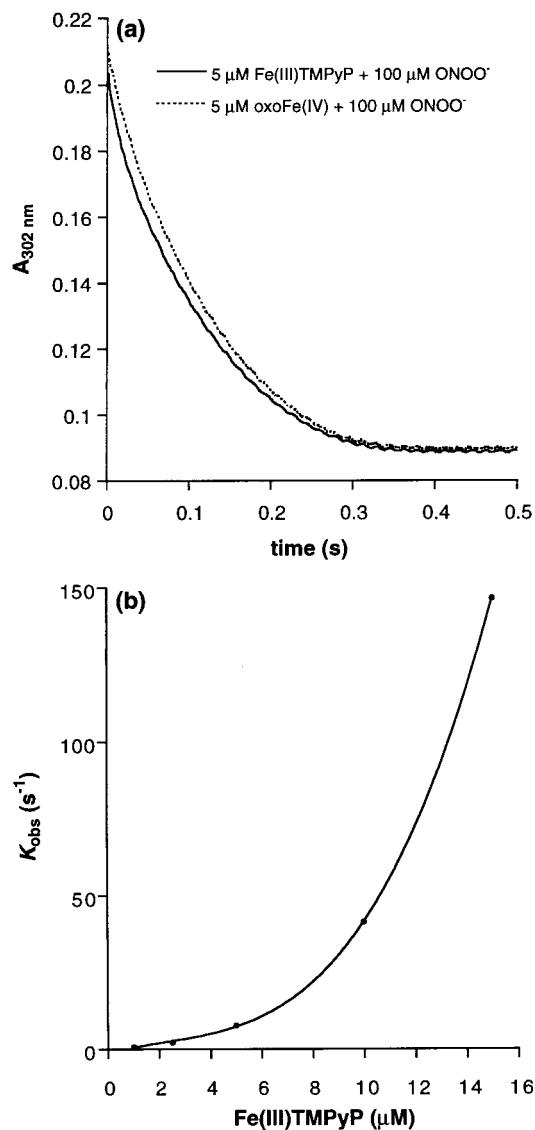
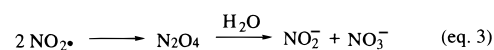


Figure 4. (a) Overlay of two kinetic traces of ONOO^- decay monitored at 302 nm. The solid trace shows decomposition of $100 \mu\text{M}$ ONOO^- in the presence of $5 \mu\text{M}$ Fe(III)TMPyP. The dotted trace shows a double-mixing experiment in which the oxoFe(IV) species was generated by reaction of $5 \mu\text{M}$ Fe(III)TMPyP with $5 \mu\text{M}$ HSO_5^- in the first mixing step, then $100 \mu\text{M}$ ONOO^- was added in the second mixing-step. (b) Dependence of the rate of ONOO^- decomposition on the concentration of Fe(III)TMPyP in 25 mM phosphate buffer at pH 7.4, 25 °C. The decay of ONOO^- was followed at 302 nm by stopped-flow spectrophotometry. The concentration of ONOO^- was kept constant ($50 \mu\text{M}$), and the concentration of Fe(III)TMPyP was varied ($1\text{--}15 \mu\text{M}$). The first-order rate constants, k_{obs} (s^{-1}), were estimated by fitting the kinetic traces into single-exponential expressions.

NO_2 ; subsequent rapid dimerization of NO_2 to N_2O_4 ($k = 9 \times 10^8 \text{ M}^{-1} \text{ s}^{-1}$)⁸⁷ would be followed by hydrolysis to 1 equiv of NO_2^- and 1 equiv of NO_3^- (eq 3), $7 \times 10^5 \text{ M}^{-1} \text{ s}^{-1}$ overall.^{87b}



Once the oxoFe(IV) species is formed, the second and slower pathway (Scheme 1, path 2) would become the active catalytic process, resulting in the conversion of ONOO^- to NO_3^- . This second catalytic pathway would explain the observation that

(87) (a) Forni, L. G.; Mora-Arellano, V. O.; Packer, J. E.; Willson, R. L. *J. Chem. Soc., Perkin Trans. 2* **1986**, 1–5. (b) Cape, J. N.; Storetonwest, R. L.; Devine, S. F.; Beatty, R. N.; Murdoch, A. *Atmos. Environ.* **1993**, *27*, 2613–21.

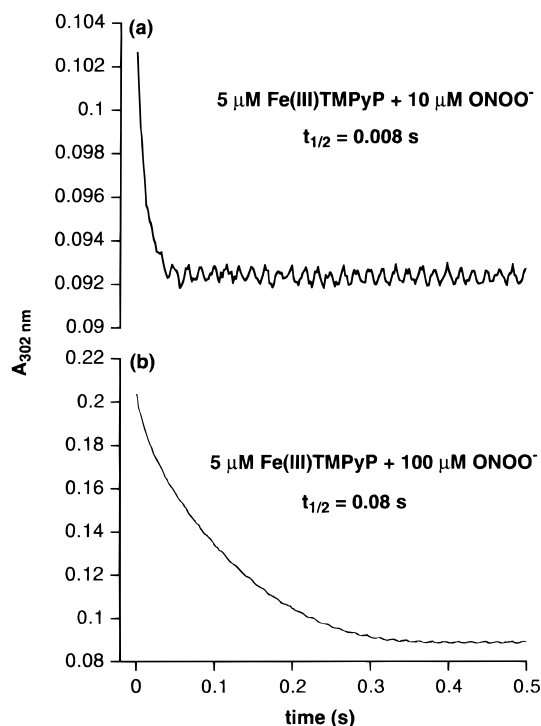
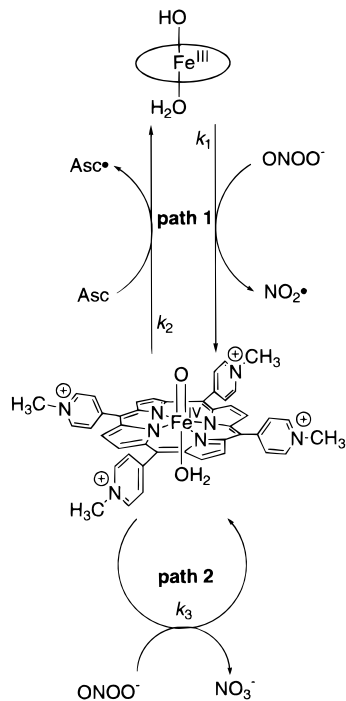


Figure 5. Decomposition of (a) 10 μM and (b) 100 μM ONOO^- catalyzed by 5 μM Fe(III)TMPyP in 25 mM phosphate buffer at pH 7.4, 25 $^\circ\text{C}$. The decay of ONOO^- was followed at 302 nm.

Scheme 1. A Simplified Mechanism of the Fe(III)TMPyP -Catalyzed Decomposition of ONOO^- , Which Consists of Two Catalytic Cycles^a



^a The fast cycle (path 1) involves Fe(III) as the active catalyst; the slower cycle (path 2) involves oxoFe(IV) species as the active catalyst.

NO_3^- is the main product in the iron porphyrin-catalyzed decomposition of ONOO^- .⁵⁹ In fact, the $\text{NO}_2^-/\text{NO}_3^-$ ratio was found to be lower for the more reactive porphyrin, Fe(III)TMPyP , than for a less reactive porphyrin, Fe(III)TMPS , presumably because the oxoFe(IV) pathway (path 2) was more

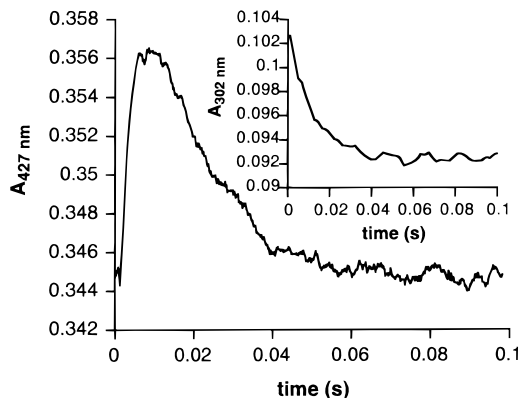


Figure 6. Formation and decay of reactive intermediate **I** (see Scheme 2) in the reaction of 5 μM Fe(III)TMPyP and 10 μM ONOO^- , monitored at 427 nm. Fitting the decay to a single exponential gave $62.2 \pm 0.8 \text{ s}^{-1}$ ($R = 0.993$). Inset: Simultaneous decay of ONOO^- , monitored at 302 nm, in the same reaction.

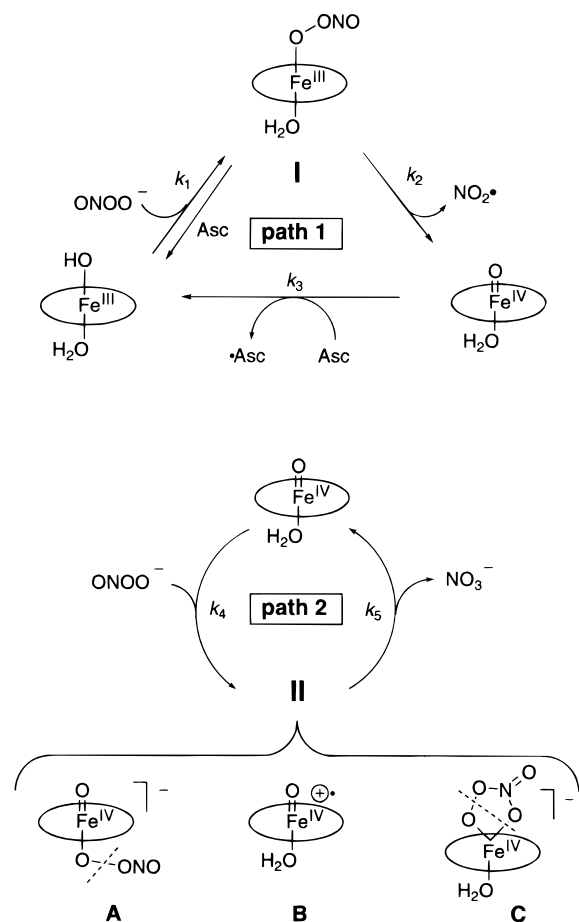
dominant in the former case, and thus more NO_3^- was produced.^{59,85}

When ONOO^- is under pseudo-first-order conditions relative to the concentration of Fe(III)TMPyP , the two catalytic processes depicted in Scheme 1 could collapse into an apparent single pathway in which the oxoFe(IV) catalytic pathway (path 2) predominates. The initial reservoir of Fe(III)TMPyP would be quickly depleted by the first equivalent of ONOO^- during the dead time of our stopped-flow instrument, as was observed. In the subsequent catalytic reaction, the oxoFe(IV) intermediate would thus be the active species that isomerized the bulk of the ONOO^- to NO_3^- . This would explain why the two traces in Figure 4a overlay so well, and why the correlation in Figure 4b at low Fe(III)TMPyP concentrations is nearly linear with an estimated $k_{\text{cat}} = 1.8 \times 10^6 \text{ M}^{-1} \text{ s}^{-1}$ for path 2. However, the contribution of the fast pathway (path 1) would become significant when the concentrations of Fe(III)TMPyP and ONOO^- are near stoichiometric (Figure 5a). Further, as shown in Scheme 1, the presence of ascorbate would short-circuit the slow pathway (path 2), making the fast pathway dominant by reducing oxoFe(IV) back to Fe(III) . The rate of oxoFe(IV) reduction by ascorbate was estimated to be approximately $2 \times 10^8 \text{ M}^{-1} \text{ s}^{-1}$ (data not shown), which is similar to the rate of oxoMn(IV) reduction by ascorbate.^{54,55} Not surprisingly, the k_{cat} for the catalyzed ONOO^- decomposition in the presence of physiologically significant concentrations of ascorbate has been estimated to be $> 10^7 \text{ M}^{-1} \text{ s}^{-1}$,⁸⁶ which is much faster than that in the absence of ascorbate which can reduce both oxoFe(IV) and intermediate **I**. Also consistent with the mechanism shown in Scheme 1, the yield of NO_2^- increased significantly under these reducing conditions.⁸⁶

Intermediates and Mechanisms of Fast and Slow Pathways. The simplified mechanism in Scheme 1 gives an overall picture of Fe(III)TMPyP -catalyzed decomposition of ONOO^- . However, the detailed mechanisms require further elaboration, since it became apparent during the course of our investigation that additional intermediates were involved.

When Fe(III)TMPyP was allowed to react with near stoichiometric amounts of ONOO^- , a new reactive intermediate, **I**, was detected (Figure 6). As determined by monitoring the Soret λ_{max} at 427 nm, intermediate **I** was formed and reached a steady state during the course of ONOO^- decomposition (Figure 6). The formation rate of intermediate **I** was very rapid, with an estimated second-order rate constant faster than $5 \times 10^7 \text{ M}^{-1} \text{ s}^{-1}$. Interestingly, the half-life of intermediate **I** ($\approx 10 \text{ ms}$)

Scheme 2. Proposed Mechanisms and Intermediates in the Fast (path 1) and Slow (path 2) Cycles of the Fe(III)TMPyP-Catalyzed Decomposition of ONOO⁻



coincides with that of ONOO⁻ (≈ 8 ms; Figure 6, inset, and Figure 5a), suggesting that the decay of **I** is the rate-limiting step under these conditions. A likely candidate for intermediate **I** is a 1:1 adduct of Fe(III)TMPyP and ONOO⁻ (see Scheme 2, path 1). Ligand exchange to form the Fe(III)TMPyP–ONOO⁻ adduct is expected to be fast, and cleavage of the adduct to produce oxoFe(IV) and NO₂ would thus be rate-limiting. The apparent first-order rate constant for the decay of intermediate **I**, determined by fitting of the trace shown in Figure 6 to a single-exponential decay, was 62.2 s^{-1} .

A second intermediate, **II**, was detected when excess ONOO⁻ (100 μM) reacted with Fe(III)TMPyP (5 μM) under pseudo-first-order conditions (Figure 7a). The formation and decay of intermediate **II** were much slower than those of intermediate **I**. Significantly, intermediate **II** reached a steady state as ONOO⁻ was disappearing via the slower path 2, and this steady state was followed by the decay of **II** to the oxoFe(IV) species. Estimation of the decay rate of **II** back to oxoFe(IV) was not straightforward, as the kinetics of this decay overlapped with the decay of oxoFe(IV) to Fe(III)TMPyP. Nevertheless, under these pseudo-first-order conditions, the decay of intermediate **II** was almost as fast as the disappearance of ONOO⁻, which had an apparent first-order rate of 13.1 s^{-1} under these conditions (see Figure 5b for a representative trace). Therefore, the turnover of the catalytic cycle (path 2) appeared to be limited by the decay rate of intermediate **II**.

Under conditions of excess ONOO⁻, intermediate **I** would be fully formed during the dead time of our stopped-flow instrument. Intermediate **I** would then decay rapidly to oxoFe-

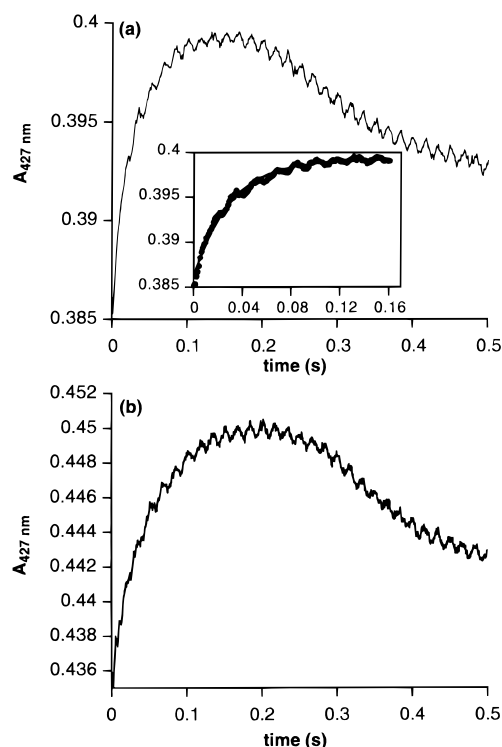


Figure 7. (a) Formation of reactive intermediate **II** (see Scheme 2) in the reaction of 5 μM Fe(III)TMPyP and 100 μM ONOO⁻, monitored at 427 nm. Inset: Kinetic profile of the formation of intermediate **II** fitted to a single-exponential curve, providing a first-order rate constant of $33.7 \pm 0.7 \text{ s}^{-1}$ ($R = 0.994$). (b) Formation of reactive intermediate **II** in a double-mixing stopped-flow experiment, in which the oxoFe(IV) species was generated in the first-mixing step by reaction of 5 μM Fe(III)TMPyP with 5 μM HSO₅⁻, and 100 μM ONOO⁻ was added in the second mixing step.

(IV), which would be captured by excess ONOO⁻ to form intermediate **II**. Thus, the rate of formation of intermediate **II** should be limited by the decay of **I**. Indeed, the rate of intermediate **II** formation was estimated to be about 33.7 s^{-1} under these conditions (Figure 7a, inset), which was comparable to but slower than the decay rate observed for intermediate **I** (62.2 s^{-1}).

To confirm that intermediate **II** was produced from a reaction of oxoFe(IV) and ONOO⁻, the oxoFe(IV) species was prepared independently by the stoichiometric reaction of Fe(III)TMPyP (5 μM) and HSO₅⁻ (5 μM). Subsequent addition of ONOO⁻ (100 μM) under pseudo-first-order conditions afforded the same intermediate **II** (Figure 7b), with exactly the same kinetic behavior as the intermediate in the direct reaction of Fe(III)TMPyP and ONOO⁻.

The exact identity of intermediate **II** is not clear from the information at hand, though several possible candidates are shown in Scheme 2 (structures **A**, **B**, and **C**). Structure **A** is a ligation adduct of ONOO⁻ and oxoFe(IV), and the similarity of the visible spectrum of **II** and oxoFe(IV) supports this structural assignment for **II**. Adduct **A** could decompose to an oxoFe(IV) porphyrin cation radical species and NO₂ by homolysis of the oxoFe(IV)-bound ONOO⁻. Subsequent rebound of NO₂ with the oxoFe(IV) porphyrin cation radical would produce NO₃⁻ and oxoFe(IV), thus completing the catalytic cycle of path 2.

The second candidate for intermediate **II** is structure **B**, the oxoFe(IV) porphyrin cation radical itself [or oxoFe(V)], possibly formed by homolysis of the O–O bond in structure **A**, with concurrent formation of an equivalent of NO₂. However, the

similarity of the visible spectrum of **II** and oxoFe(IV) makes structure **B** a less likely intermediate than **A** or **C**. Reduction of intermediate **II-B** by NO_2^- to give the oxoFe(IV) porphyrin and NO_2 is expected to be very fast, by analogy to the rapid reduction of oxoMn(V) by NO_2^- .⁸³ Thus, NO_2^- (generated via eq 3) could be recycled to NO_2 during the catalytic turnover, and this NO_2 would then generate more NO_2^- and NO_3^- . Eventually, in this scenario, all the NO_2 produced from the decomposition of intermediate **II** would be converted to NO_3^- , as is observed.

The third candidate for intermediate **II**, structure **C**, could be produced by cyclic addition of ONOO^- to oxoFe(IV) from the metal-oxo face of the porphyrin. Structure **C** is a complex of the Fe(IV) porphyrin and peroxyxynitrate (O_2NOO^-); O_2NOO^- is a known compound that has been prepared previously.⁸⁸ Further, an analogous bidentate nitrate iron porphyrin complex has been characterized by X-ray crystallography.⁸⁹ Decomposition of the O_2NOO^- -Fe(IV) porphyrin complex **C** would produce NO_3^- and oxoFe(IV). Interestingly, this pathway would be available to heme proteins such as myeloperoxidase, which are known to produce oxoFe(IV) intermediates in which one axial iron position is blocked by imidazole ligation.^{10,77} Significantly, all three of the postulated candidates for intermediate **II** would lead to the production of NO_3^- as the major product, consistent with the observed results.⁵⁹

Fe(III)TMPyP as Superoxide Dismutase Mimics. Fe(III)-TMPyP has been shown to possess modest SOD activity by indirect assay, with $k_{\text{cat}} \sim 10^7 \text{ M}^{-1} \text{ s}^{-1}$.⁹⁰⁻⁹² We have directly evaluated the SOD activity of Fe(III)TMPyP for the first time by following the decay of $\text{O}_2^{\bullet-}$ using a specialized four-syringe setup of the stopped-flow spectrophotometer that we have recently described.^{54,55,83} Reproducibly, the self-dismutation of $\text{O}_2^{\bullet-}$ in pH 7.4 phosphate buffer was found to be second order in $\text{O}_2^{\bullet-}$, with a rate constant around $7.3 \times 10^5 \text{ M}^{-1} \text{ s}^{-1}$ in this apparatus, as expected from published results (Figure 8a).⁵⁵ Fe(III)TMPyP at low concentrations significantly accelerated the dismutation of $\text{O}_2^{\bullet-}$ (Figure 8b). As we have recently described for Mn(III)TMPyP,⁵⁵ the apparent first-order rate constants (k_{obs}) of Fe(III)TMPyP-catalyzed dismutation of $\text{O}_2^{\bullet-}$ were extracted by nonlinear least-squares fitting of the experimental data into eq 4, taking into consideration both self-dismutation and Fe(III)TMPyP-catalyzed dismutation, which significantly improved the fit of the data.

$$[\text{O}_2^{\bullet-}] = \frac{[\text{O}_2^{\bullet-}]_0 k_{\text{obs}} \exp(-k_{\text{obs}} t)}{k_{\text{obs}} + k_{\text{self}} [\text{O}_2^{\bullet-}]_0 (1 - \exp(-k_{\text{obs}} t))} \quad (4)$$

The rate of Fe(III)TMPyP-catalyzed dismutation of $\text{O}_2^{\bullet-}$ was estimated to be $1.9 \times 10^7 \text{ M}^{-1} \text{ s}^{-1}$, obtained from the slope of a linear plot of k_{obs} vs Fe(III)TMPyP concentrations (Figure 8b, inset). This rate is in good agreement with the results obtained by indirect assay.⁹⁰⁻⁹² The mechanism of Fe(III)TMPyP-catalyzed dismutation of $\text{O}_2^{\bullet-}$ is similar to that of Mn(III)TMPyP: reduction of Fe(III)TMPyP to Fe(II)TMPyP by $\text{O}_2^{\bullet-}$ is rate limiting, followed by fast oxidation of Fe(II) back to Fe(III) by $\text{O}_2^{\bullet-}$ at a near diffusion-controlled rate ($\sim 4.2 \times 10^9 \text{ M}^{-1} \text{ s}^{-1}$).⁹³

(88) Løgager, T.; Sehested, K. *J. Phys. Chem.* **1993**, *97*, 10047-10052.

(89) Philippi, M. A.; Baenziger, N.; Goff, H. M. *Inorg. Chem.* **1981**, *20*, 3904-3911.

(90) Pasternack, R. F.; Halliwell, B. *J. Am. Chem. Soc.* **1979**, *101*, 1026-1031.

(91) Pasternack, R. F.; Skowronek, W. R. *J. Inorg. Biochem.* **1979**, *11*, 261-267.

(92) Ilan, Y.; Rabani, J.; Fridovich, I.; Pasternack, R. F. *Inorg. Nucl. Chem. Lett.* **1981**, *17*, 93-96.

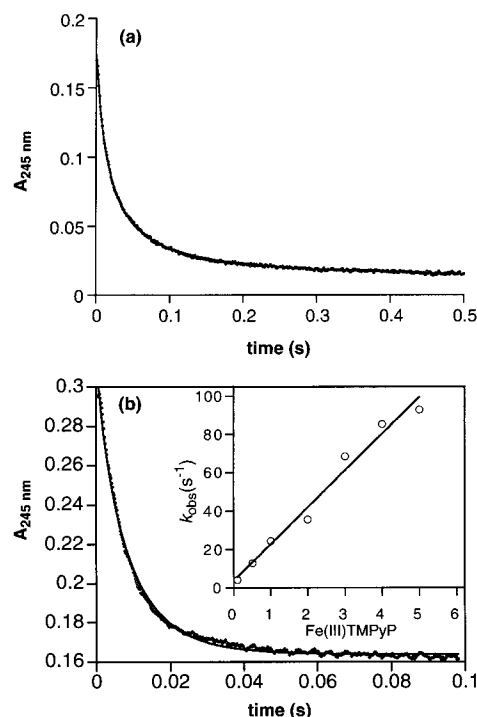
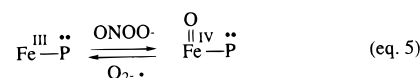


Figure 8. Decay of $\text{O}_2^{\bullet-}$ in 25 mM phosphate buffer at pH 7.4, 25 °C (a) in the absence of porphyrin catalyst and (b) in the presence of 5 μM Fe(III)TMPyP. The solid lines overlaid on the two traces are the nonlinear least-squares fitting of the experimental data to (a) second-order kinetics ($R = 0.999$) and (b) eq 4 ($R = 0.998$). Inset: Linear least-squares fit of the pseudo-first-order rate constants vs Fe(III)TMPyP concentration gives $k_{\text{cat}} = 1.9 \times 10^7 \text{ M}^{-1} \text{ s}^{-1}$ ($R = 0.989$).

As we have recently described for Mn(III)TMPyP,⁵⁵ the powerful reducing ability of $\text{O}_2^{\bullet-}$ offers the opportunity for $\text{O}_2^{\bullet-}$ not only to reduce Fe(III)TMPyP to the Fe(II) species, but also to very rapidly reduce the oxoFe(IV) species to Fe(III). This rapid reduction of the oxoFe(IV) species by $\text{O}_2^{\bullet-}$ would short-circuit path 1 of Fe(III)TMPyP-catalyzed decomposition of ONOO^- (see Schemes 1 and 2), by analogy with the ascorbate reduction described above. Thus, the process for simultaneous removal of ONOO^- and $\text{O}_2^{\bullet-}$ that we have described for Mn(III)TMPyP⁵⁵ would also be available to Fe(III)TMPyP. The known Fe(III)-Fe(II) dismutation cycle would thus be supplemented by the oxoFe(IV)-Fe(III) ONOO^- reductase cycle, shown in eq 5.



More significantly, the fast reduction of oxoFe(IV) species by $\text{O}_2^{\bullet-}$ would make the fast path for ONOO^- reaction (path 1, see Schemes 1 and 2) the major contributor to the activity of Fe(III)TMPyP as a ONOO^- decomposition catalyst.

Conclusions

The reactions of Fe(III)TMPyP with ONOO^- are much more complex than the analogous reactions of Mn(III)TMPyP.^{54,55} We have discovered that two different processes operate in FeTMPyP-catalyzed decomposition of ONOO^- . A fast and stoichiometric pathway involving Fe(III)TMPyP as the active species will dominate when the ONOO^- concentration is

(93) Faraggi, M. *O₂^{•-} dismutation catalyzed by water soluble porphyrins. A pulse radiolysis study*; Bors, W., Saran, M., Tait, D., Eds.; Walter de Gruyter: Berlin, 1984; pp 419-430.

comparable to or lower than that of Fe(III)TMPyP. A 10-fold slower catalytic pathway involves oxoFe(IV)TMPyP as the active species when ONOO⁻ is in excess (Schemes 1 and 2). Which pathway dominates the ONOO⁻ decomposition is highly dependent on the reaction conditions (e.g., the relative concentrations of iron catalyst and ONOO⁻, the presence or absence of reducing agents such as biological antioxidants or O₂^{-•}). The two pathways are certainly connected by oxoFe(IV) intermediates; however, it is not clear if they are also interconnected by any other means.

Further, the presence of antioxidants *in vivo* and O₂^{-•} under oxidative stress conditions may allow the faster Fe(III) pathway (path 1) to be the dominant mode of ONOO⁻ decomposition catalyzed by Fe(III)TMPyP. Thus, the activity of Fe(III)TMPyP *in vivo* would be expected to be higher than that *in vitro* when reducing agents are absent.

Finally, the SOD-mimetic activity that we have measured for Fe(III)TMPyP allows this catalyst to perform simultaneously as a O₂^{-•} dismutase and a ONOO⁻ isomerase. Given the excellent reducing ability of O₂^{-•}, the concerted removal of *both* O₂^{-•} and ONOO⁻, mediated by the potential O₂^{-•}-coupled ONOO⁻ reductase⁵⁵ activity of Fe(III)TMPyP, may be a significant component of the biological activity that this and other iron porphyrins have shown⁵⁹ in ONOO⁻-related disease states.

Experimental Section

Materials. 5,10,15,20-Tetrakis(*N*-methyl-4'-pyridyl)porphyrinatoiron(III) chloride [Fe(III)TMPyP(Cl)] was purchased from Mid-Century Chemical. Anhydrous monosodium phosphate and anhydrous disodium phosphate were purchased from Sigma. Sodium L-ascorbate, potassium superoxide (KO₂), potassium peroxymonosulfate (HSO₅⁻), and 3-chloroperoxybenzoic acid (*m*-CPBA) were obtained from Aldrich. Peroxynitrite was prepared from the reaction of acidic H₂O₂ with sodium nitrite following the published procedure.⁵³ All the solvents were analytical grade. Dry DMSO was distilled under reduced pressure from calcium hydride. Water used in all the experiments was distilled and deionized (Millipore, Milli-Q).

Time-Resolved Visible Spectra. All the time-resolved visible spectra were recorded on a HI-TECH SF-61 DX2 stopped-flow spectrophotometer with use of the photodiode array fast-scan mode. The spectral resolution was about 1 nm. Reactions between Fe(III)-TMPyP and oxidants (*m*-CPBA, ONOO⁻) were single-mixing experiments, and the concentrations presented in all cases are the final

concentrations after mixing. The porphyrin solutions were buffered with 50 mM sodium phosphate, pH 7.4. The same reactions were also performed in the presence of NaNO₂ in the case of *m*-CPBA as the oxidant.

Reaction Kinetics. Reaction kinetic profiles were collected in the photomultiplier mode on the HI-TECH SF-61 DX2 stopped-flow spectrophotometer (1 ms dead time) by using single- or double-mixing modes. The kinetic profiles of Fe(III)TMPyP-catalyzed decomposition of ONOO⁻ in 25 mM phosphate pH 7.4 buffer at 25 °C were monitored at 302 nm. The generation and the decay of intermediates were followed at 427 nm.

The reduction rates of oxoFe(IV) species by NaNO₂ and ascorbate were measured directly by performing double-mixing experiments: The oxoFe(IV) intermediates were fully generated during the first mixing step by the stoichiometric reaction of Fe(III)TMPyP (5 μM) and HSO₅⁻ (5 μM), followed by the addition of NaNO₂ (0.5–50 mM) or ascorbate (5 μM) in the second mixing step. To examine the reactivity of the oxoFe(IV) species toward ONOO⁻, the oxoFe(IV) was similarly prepared in the first mixing step, followed by addition of ONOO⁻ (100 μM) in the second mixing step.

Superoxide Dismutation. A DMSO solution of KO₂ (~2 mM) was prepared following the published procedure.⁹⁴ The dismutation of O₂^{-•} was monitored directly at the O₂^{-•} absorbance (245 nm), using a special setup of the four-syringe, double-mixing sample handling unit to reduce changes in the refractive index due to the mixing of DMSO and buffer. In this stopped-flow setup, the KO₂/DMSO solution was loaded in syringe A (0.5 mL) and 50 mM pH 7.4 phosphate buffer was loaded in syringes B (2.5 mL), C (0.5 mL), and D (2.5 mL). Syringes A, B, C, and D were labeled from left to right. All four syringes were pushed up simultaneously by the extended plate; the contents of syringes A and B were first mixed in an aging loop, and then mixed with the contents of syringes C and D. A 12-fold dilution of the KO₂/DMSO solution was achieved with this two-stage mixing, thus minimizing the interference due to DMSO/water interaction. In the SOD activity assays, iron porphyrin solutions were loaded into syringe C.

Acknowledgment. Support of this research by the National Institutes of Health (GM36928), the National Science Foundation for the purchase of 500 and 600 MHz NMR spectrometers, and Princeton University for the purchase of a stopped-flow spectrophotometer are gratefully acknowledged. J.A.H. is the recipient of an NIH NRSA fellowship (GM18490).

JA980507Y

(94) Riley, D. P.; Rivers, W. J.; Weiss, R. H. *Anal. Biochem.* **1991**, *196*, 344–349.